CivilEng

MDPI

Article

Simplified Method for Determining Thermal Stresses during the Construction of Massive Monolithic Foundation Slabs

Anton Chepurnenko [1,*] and Vasilina Turina [2]

[1] Strength of Materials Department, Faculty of Civil and Industrial Engineering, Don State Technical University, 344003 Rostov-on-Don, Russia
[2] Technical Mechanics Department, Faculty of Civil and Industrial Engineering, Don State Technical University, 344003 Rostov-on-Don, Russia; vasilina.93@mail.ru
* Correspondence: anton_chepurnenk@mail.ru; Tel.: +7-863-201-9136

Abstract: For massive monolithic foundation slabs, the problem of early cracking due to the intense heat release of concrete during the hardening process is relevant. The purpose of this article is to develop a simplified method for determining thermal stresses during the construction of massive monolithic foundation slabs. The proposed technique is based on the hypothesis of parabolic temperature distribution over the thickness of the structure at each moment of time. In addition to the parabolic distribution, the half-wave cosine distribution is also used. A hypothesis is also introduced about the same conditions of heat exchange with the environment on the lower and upper surfaces of the foundation. As a result, formulas are obtained that establish a direct relationship between thermal stresses and the temperature difference between the center and the surface. The solution to the test problem for the foundation slab is presented and compared with an alternative technique that does not use the hypothesis about the character of the temperature distribution over the thickness. Also, the inverse problem of determining the allowable temperature drop between the center and the surface of the structure is solved, at which the stresses on the upper surface at each moment of time will not exceed the tensile strength of concrete.

Keywords: reinforced concrete; foundation slab; temperature stresses; internal heat release; early age cracking

Citation: Chepurnenko, A.; Turina, V. Simplified Method for Determining Thermal Stresses during the Construction of Massive Monolithic Foundation Slabs. *CivilEng* **2023**, *4*, 740–752. https://doi.org/10.3390/civileng4030042

Academic Editors: Patrick Dangla and Angelo Luongo

Received: 23 April 2023
Revised: 25 May 2023
Accepted: 27 June 2023
Published: 3 July 2023

1. Introduction

Concrete is a durable and reliable material, which is one of the most commonly used in construction today throughout the world. Reinforced concrete structures have many positive qualities, including high load-bearing capacity, durability, fire resistance, etc. Concrete also has a competitive price due to the possibility of using local raw materials. However, concrete is characterized by volumetric instability in the hardening phase, due to temperature effects and shrinkage, which is one of its unfavorable properties [1]. Volumetric instability and a tendency to early cracking are exacrbated in massive structures made from concretes with a low water–cement ratio and a high cement content [2]. Early cracking leads to the fact that water and aggressive ions can penetrate the cracks, which causes a loss of functionality, durability and aesthetics. Cracks that have arisen at the hardening stage also lead to a decrease in the rigidity and bearing capacity of reinforced concrete structures [3]. In some cases, intense cracking at the stage of hardening may even call into question the possibility of further operation of structures [4].

Monolithic foundation slabs are one of the widely used types of massive reinforced concrete structures. The massiveness of the structure predetermines the need to develop special technological solutions to control the parameters of heat and mass transfer, the rate of concreting, as well as the selection of concrete mix formulations to eliminate the risk of early cracking [5]. The choice of rational technological solutions can be carried out based on computer simulation methods [6]. The solution to the problem of determining

the stress–strain state in massive monolithic reinforced concrete structures during the construction process requires the calculation of a non-stationary temperature field in the presence of internal sources of heat release, as well as taking into account the dependence of material characteristics on time when calculating internal stresses [7].

The problem associated with the cracking of hardening concrete structures caused by the heat of hydration has long been known. This problem has been around for probably as long as concrete has been used as a building material [8]. During the construction of massive dams, this was especially noticeable in the first days after their concreting [9].

It is known that thermal stresses leading to cracking occur only in the presence of deformation constraints. These restraints can be divided into internal and external [5,10]. Internal restraints are due to the fact that with uneven heating, each elementary layer of the slab tends to obtain its own thermal deformation. At the same time, each vertical section of the slab must remain plane, i.e., total deformation, which is the sum of thermal deformation and deformation caused by thermal stresses, must be constant throughout the thickness of the slab. Therefore, to equalize the total deformation, tensile stresses will appear on the surfaces of the slab, and compressive stresses in the middle.

Tensile stresses on the slab surfaces will lead to surface cracks. These cracks tend to close later in the cooling phase when the core also cools down [11], but they are nonetheless the initial damage that reduces the bearing capacity of the structure and acts as a weak point for further climatic influences.

External restraints are usually associated with the construction of working seams, i.e., when the hardening structure is limited in deformation by rigid, already-hardened adjacent structural elements [12]. The classic example is a wall placed on a rigid base/slab. During the cooling phase, the wall tends to shrink in size, but it is limited by a rigid base. The stresses that arise in this situation are usually longitudinal.

The first step in the analysis of the stress–strain state of massive monolithic foundation slabs is the calculation of the temperature field caused by internal heat sources. A significant number of publications are devoted to the solution of this problem.

The main tool in determining the temperature fields in the construction of massive monolithic structures is currently the finite element method. Finite element modeling shows good agreement with the results of field temperature measurements [7].

As for the determination of thermal stresses caused by the heat release of concrete and the heat exchange of the structure with the environment, two approaches should be distinguished here. The first approach involves finite element modeling in ready-made software products (Midas Civil, ANSYS, Abaqus, etc.) and is used, for example, in [6,13,14]. However, in ready-made FEM complexes, it is not possible to take into account the change in the physical and mechanical characteristics of concrete over time, as well as to take into account the shrinkage of concrete, and the results will only be of an estimated nature.

The second approach involves determining thermal stresses using a simplified formula [15–17]:

$$\sigma(t) = k_T E(t) \alpha \Delta T, \quad (1)$$

where k_T is the restraint coefficient, E is the modulus of elasticity of concrete, α is the coefficient of linear thermal expansion, and ΔT is the temperature difference between the center and the surface of the structure.

This approach is applicable only to objects such as foundation slabs and walls. It does not allow taking into account the fact that the stress state can be biaxial or triaxial. In addition, the question arises of determining the coefficient k_T, which depends on the rigidity of the base, the dimensions of the structure being concreted, and many other factors.

Another way to monitor the structural health of building structures is machine learning methods, in particular artificial neural networks [18]. However, their use requires a large experimental base for training. Currently, the existing experimental data on temperature fields and stresses in massive monolithic foundation slabs are still insufficient.

Ref. [19] propose a method for determining thermal stresses in massive monolithic foundation slabs caused by internal restraint. It is assumed that the friction forces along

the base of the foundation do not have a noticeable effect on the stress–strain state. To confirm the reliability of the method, a comparison is carried out by [19], with the results of finite element modeling in the ANSYS software package in a three-dimensional setting at a constant modulus of elasticity of concrete. This technique also makes it possible to take into account the time variation in the characteristics of concrete, the presence of creep and shrinkage deformations, and the coefficient of reinforcement of the structure. When taking into account the dependence of the elastic modulus of concrete on time, the picture of the stress–strain state changes significantly. The disadvantage of this technique is that it does not directly relate thermal stresses to the temperature difference between the center and the surface of the structure.

The purpose of our work is to develop a simplified method for calculating thermal stresses from the temperature difference between the center and the surface of the foundation slab based on the resolving equations obtained in [19].

2. Materials and Methods

The increment of stress for a moment of time Δt without taking into account creep and shrinkage deformations based on the technique presented in [19] is determined by the formula:

$$\Delta\sigma(z) = \frac{E(z,t)}{1-\nu}(\Delta\varepsilon - \alpha[T(z,t) - T(z,t-\Delta t)]), \quad (2)$$

where T is temperature, ν is Poisson's ratio, and $\Delta\varepsilon$ is total strain increment.

The factor $(1-\nu)$ in the denominator in Formula (1) takes into account that the concrete in the foundation slab is in conditions of biaxial tension (compression). In Formula (2), shrinkage deformation is not taken into account, since it is constant over the thickness of the slab and, in the absence of external restraints, does not cause stress.

Based on the hypothesis of plane sections, the value of $\Delta\varepsilon$ is assumed to be independent of the z coordinate and is calculated by the formula:

$$\Delta\varepsilon = \frac{\alpha\int_{-h/2}^{h/2} E(z,t)[T(z,t) - T(z,t-\Delta t)]dz}{\int_{-h/2}^{h/2} E(z,t)dz}. \quad (3)$$

The zero point of the coordinate z here, in contrast to the work by [19], is taken in the median plane of the foundation slab.

The diagram of temperature distribution and the corresponding diagram of normal stresses in the foundation slab due to its uneven heating caused by the internal heat release of concrete and heat exchange with the environment are shown in Figure 1.

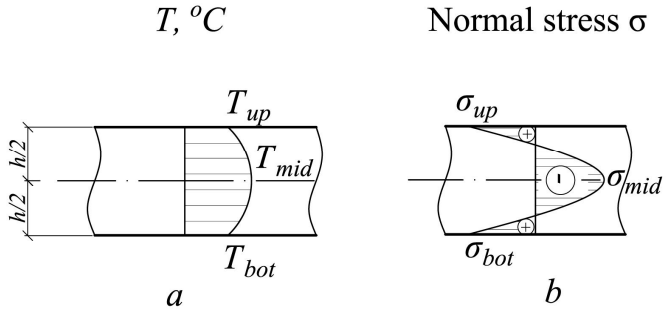

Figure 1. Diagrams of temperature (**a**) and temperature stresses (**b**) distribution in the foundation slab.

To obtain a simplified dependence that establishes a relationship between thermal stresses and the temperature difference between the center and the surface of the structure, the temperature distribution over the thickness at each moment of time will be taken according to the parabolic law:

$$T(z) = Az^2 + Bz + C. \quad (4)$$

The assumption is also introduced that the heat transfer conditions on the upper and lower surfaces of the slab are the same, i.e.,

$$T(h/2) = T(-h/2) = T_{up}. \tag{5}$$

Substitution of condition (5) into (4), as well as the condition $T(0) = T_{\text{mid}}$, allows us to determine the constants A, B and C and write the law of temperature change across the plate thickness in the form:

$$T(z) = -\frac{4z^2}{h^2}\left(T_{mid} - T_{up}\right) + T_{mid}. \tag{6}$$

In addition to the hypothesis about the same heat transfer conditions on the surfaces of the slab, it is also assumed that the modulus of elasticity of the slab does not change along the thickness. Then, Formula (3) will take the form:

$$\Delta\varepsilon = \frac{\alpha}{h}\int\limits_{-h/2}^{h/2}[T(z,t) - T(z,t-\Delta t)]dz. \tag{7}$$

The value $\langle T\rangle = \frac{1}{h}\int_{-h/2}^{h/2} T(z)dz$ is the average temperature over the slab thickness, so Formula (7) can be written as:

$$\Delta\varepsilon = \alpha(\langle T_t\rangle - \langle T_{t-\Delta t}\rangle). \tag{8}$$

For the law (6), the value $\langle T\rangle$ as a result of integration will take the form:

$$\langle T\rangle = \frac{2}{3}T_{mid} + \frac{1}{3}T_{up}. \tag{9}$$

As a result, the increment of the total deformation will be written in the form:

$$\Delta\varepsilon = \alpha\left(\frac{2}{3}(T_{mid}(t) - T_{mid}(t-\Delta t)) + \frac{1}{3}\left(T_{up}(t) - T_{up}(t-\Delta t)\right)\right). \tag{10}$$

Substitution of (10) into (2) allows us to obtain the following formulas for stress increments on the upper surface of the slab and in the middle of the thickness:

$$\Delta\sigma_{up} = \frac{2}{3}\cdot\frac{E(t)}{(1-\nu)}\alpha\left\{T_{mid}(t) - T_{up}(t) - \left[T_{mid}(t-\Delta t) - T_{up}(t-\Delta t)\right]\right\}; \tag{11}$$

$$\Delta\sigma_{mid} = -\frac{\Delta\sigma_{up}}{2}. \tag{12}$$

The expression in curly brackets in Formula (11) represents the increment in the temperature difference between the center and the surface of the structure over the time interval Δt.

The modulus of elasticity of concrete is determined as a function of compressive strength using the empirical formula given in [19]:

$$E(R) = 1000\frac{0.04R + 57}{1 + \frac{29}{3.8+0.8R}},\ \text{MPa} \tag{13}$$

The compressive strength of concrete is calculated as a function of its degree of maturity DM using the formula presented in [19]:

$$R = R_{28}\exp\left(0.35\left[1 - \left(\frac{15,800 - 122.5\overline{T}}{\overline{T}t}\right)^{0.55}\right]\right), \tag{14}$$

where R_{28} is the strength of concrete at the age of 28 days, $\overline{T} = DM/t$, t is the age of concrete in hours, DM is the degree of maturity of concrete, determined by the integral:

$$DM = \int_0^t T(\tau)d\tau, \tag{15}$$

where $T(\tau)$ is the concrete temperature at time τ.

The tensile strength of concrete R_t is also determined by us as a function of the compressive strength R using the formula proposed in [20]:

$$R_t = 0.29 \cdot R^{0.6}. \tag{16}$$

Poisson's ratio of concrete ν is taken constant and equal to 0.2.

3. Results and Discussion

The first stage of our study was the verification of the relations (13)–(16) on the experimental data presented by [21]. In this work, the hardening of the samples occurred with a complete limitation on their deformation, and temperature and stress measurements were performed at various points in time. The scheme of the experimental setup is shown in Figure 2.

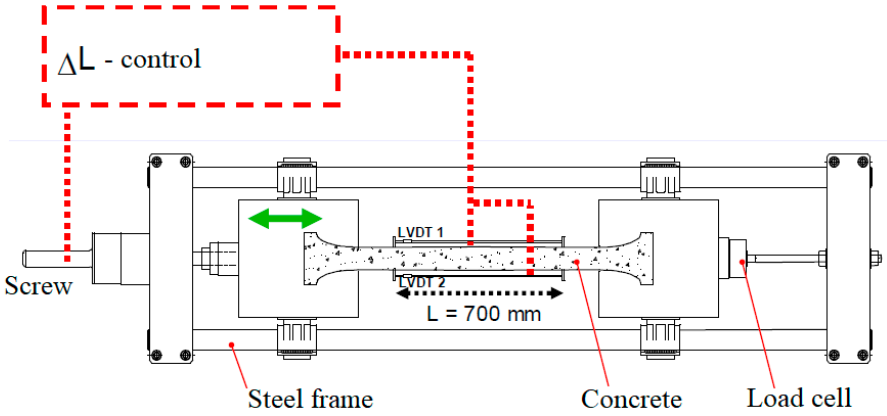

Figure 2. Scheme of tests carried out in [21].

When compared with experimental data, autogenous shrinkage deformations were also taken into account, which were determined by the formula

$$\varepsilon_{sh}(t) = -(0.2B - 2)(a \ln t - b) \cdot 10^{-5} \leq 0, \tag{17}$$

where t is time, $B = R_{28} - 12$ is the class of concrete (MPa), $a = 0.31$ and $b = 0.4$ are the empirical coefficients.

Tests in [21] were carried out for concrete specimens with strength at a design age of 28 days $R_{28} = 80$ MPa. Figure 3 shows a graph of temperature changes over time for one of the tested samples.

Figure 4 compares the stress values at different points in time, obtained experimentally, with the results of numerical simulation using relations (13)–(17). Figure 4 shows a satisfactory agreement between the experimental results and theory.

In [21], for the samples under consideration, a curve of change in tensile strength with time is also given. A comparison of the curve presented in [21] with the curve $R_t(t)$ constructed using dependences (14)–(16) is shown in Figure 5. The presented graph shows a good agreement between the results.

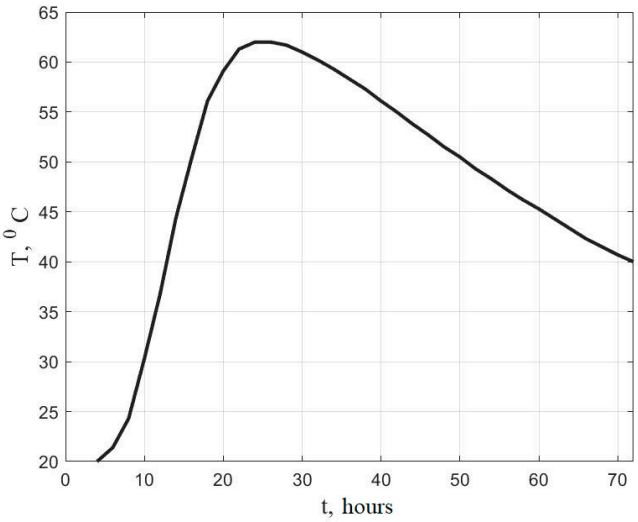

Figure 3. Change in temperature of the tested sample with time.

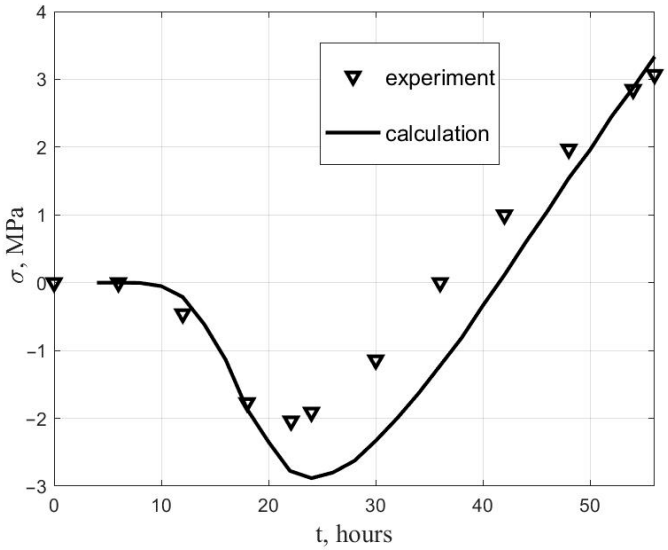

Figure 4. Comparison of experimental results with calculation results.

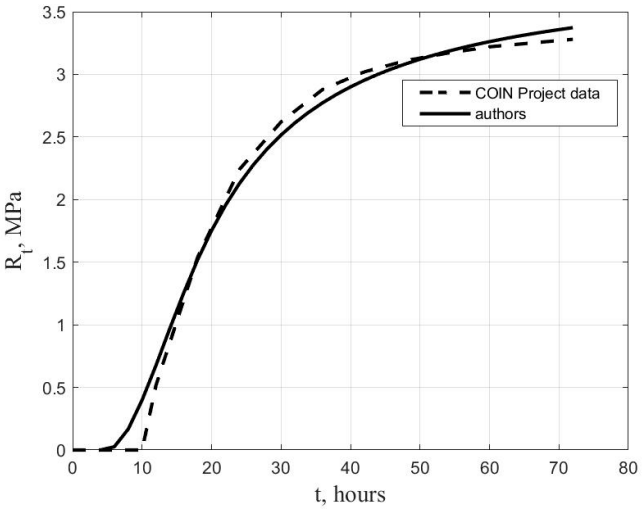

Figure 5. Comparison of the curve $R_t(t)$ given in [21] with the curve constructed by Formulas (14)–(16).

To verify the developed methodology, a test problem was also solved for a massive foundation slab 1 m thick. The initial temperature of the concrete mixture and the ambient temperature were taken equal to 20 °C, the heat transfer coefficient on the upper surface was 8 W/(m^2·°C), the thermal conductivity coefficient of concrete λ = 2.67 W/(m·°C), concrete density ρ = 2500 kg/m^3, specific heat capacity c = 1000 J/(kg·°C). The heat release function for 1 m^3 of concrete based on [22] was taken as:

$$Q(t) = Q_{28} \cdot \exp\left[k \cdot \left(1 - \left(\frac{28}{t}\right)^{x}\right)\right], \quad (18)$$

where t is time in days, Q_{28} = 130 MJ/m^3, k = 0.13, x = 0.42.

The presented parameters Q_{28}, k, x correspond to B25 class quick-hardening concrete (R_{28} = 37 MPa) according to Russian standards.

The temperature field was determined from the solution of the heat conduction differential equation by the finite element method in a one-dimensional setting according to the procedure given in [19,23]. The thickness of the slab was divided into 100 finite elements, and the number of time steps was taken equal to 800.

Figure 6 shows graphs of temperature changes over time on the surface of the structure, as well as in its center. Figures 7 and 8 show the change in time of the modulus of elasticity of concrete and its tensile strength at $z = h/2$.

Figure 9 shows the graphs of stress changes over time on the upper surface, as well as in the center of the structure. The solid lines correspond to the solution according to the method proposed in [19], and the dashed lines correspond to the simplified method. From Figure 9 it can be seen that the stresses on the upper surface first increase and then decrease and become compressive. In the center of the structure, the trend is reversed. The moment of stress growth on the upper surface corresponds to the heating of the foundation, and their decrease occurs during cooling. As a result of uneven heating of the structure during its hardening, there are always residual stresses. The character of the stress change curve in the center of the structure coincides with the experimental results presented in Figure 4.

The results obtained by the two methods are quite close. The deviations can be explained by the fact that at the initial stage, the temperature distribution over the thickness of the structure differs from parabolic (Figure 10). The advantage of the method proposed in this article is that it allows one to estimate thermal stresses directly from the temperature difference between the center and the surface of the structure, which can be measured directly at the construction site.

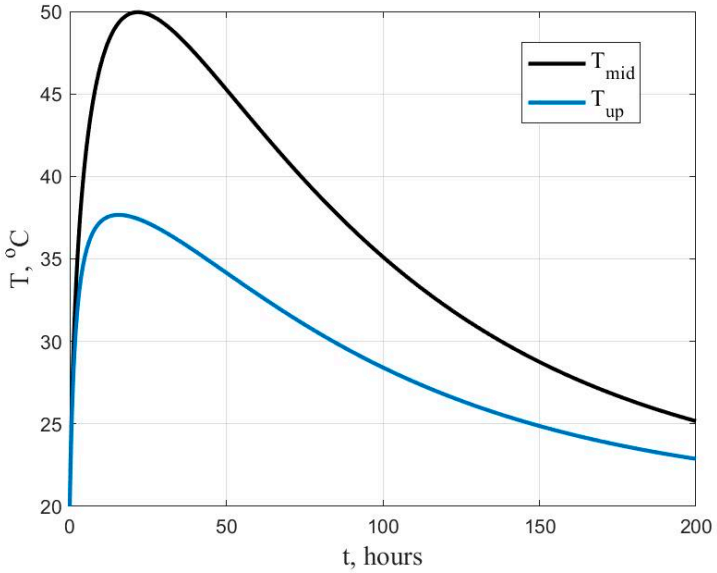

Figure 6. Temperature change over time in the center and on the surface of the structure.

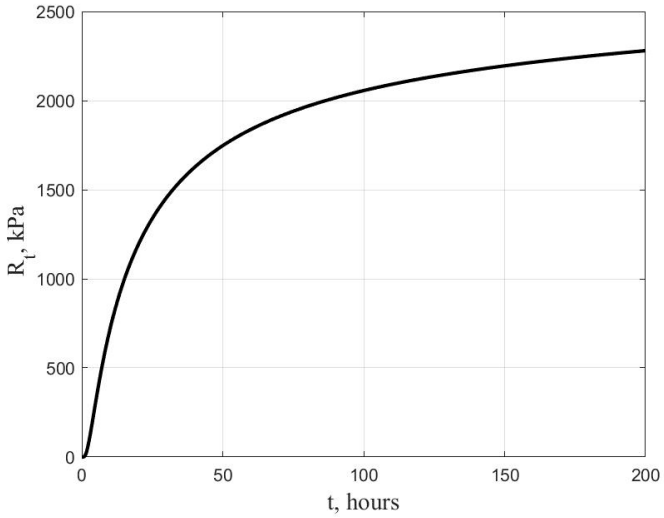

Figure 7. Change in concrete tensile strength over time at $z = h/2$.

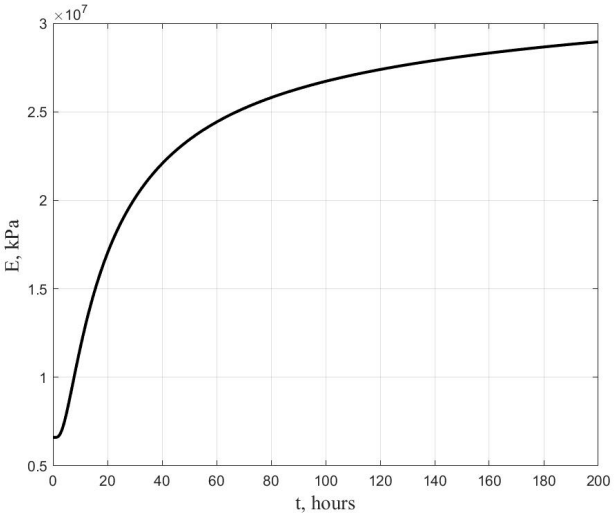

Figure 8. Change in the modulus of elasticity of concrete over time at $z = h/2$.

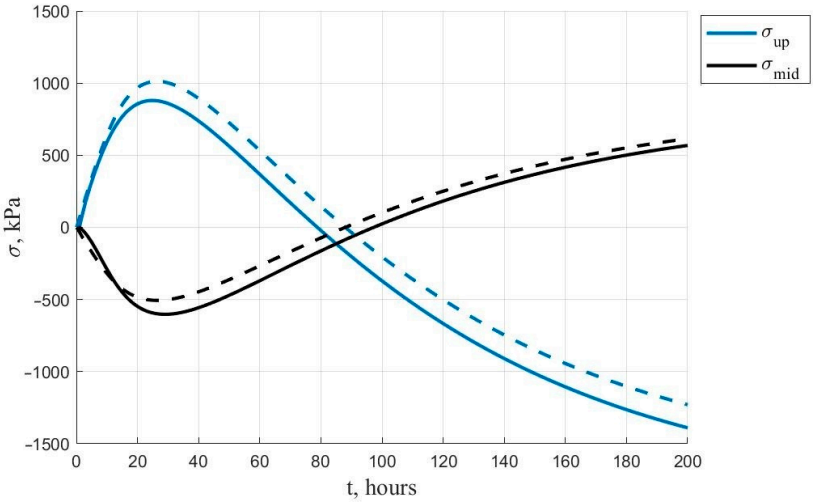

Figure 9. Change in stresses at the top surface and in the center of the structure over time: solid lines—calculation according to the method proposed in [19]; dashed lines—calculation according to the approximate method proposed in this paper.

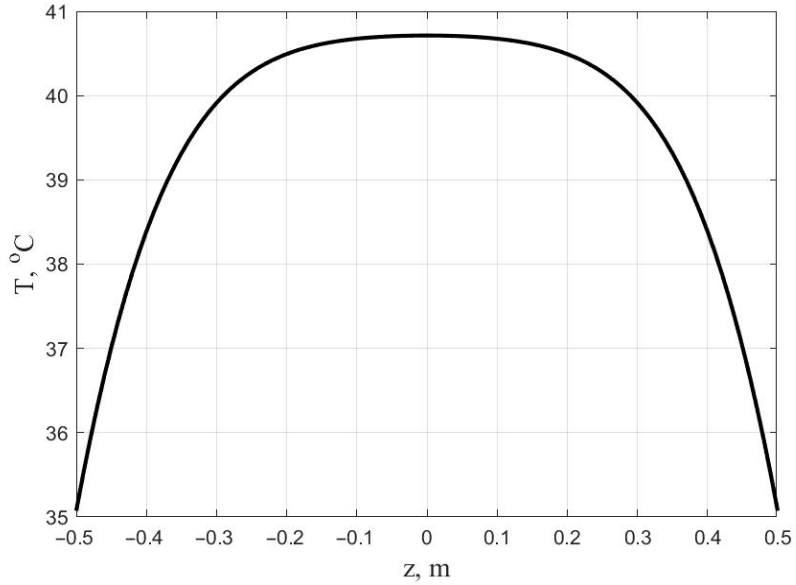

Figure 10. Temperature distribution over the slab thickness at t = 5 h.

Note that the function of temperature change with thickness in the method proposed by us can be specified not only in the form of a square parabola. So, when the distribution is given in the form of a cosine wave

$$T(z) = T_{up} + \left(T_{mid} - T_{up}\right) \cdot \cos \frac{\pi z}{h} \tag{19}$$

the average temperature over the thickness can be represented as:

$$\langle T \rangle = \omega T_{mid} + (1 - \omega) T_{up}, \tag{20}$$

where $\omega = 2/\pi$.

Then, the formulas for stress increments on the upper surface and in the center of the slab are written as:

$$\Delta\sigma_{up} = \frac{\omega \alpha E(t)}{(1-\nu)} \left\{ T_{mid}(t) - T_{up}(t) - \left[T_{mid}(t - \Delta t) - T_{up}(t - \Delta t) \right] \right\}; \tag{21}$$

$$\Delta\sigma_{mid} = \frac{(\omega - 1) \alpha E(t)}{(1-\nu)} \left\{ T_{mid}(t) - T_{up}(t) - \left[T_{mid}(t - \Delta t) - T_{up}(t - \Delta t) \right] \right\}. \tag{22}$$

Formulas (11) and (12) can also be represented as (21) and (22) if we assume $\omega = 2/3$.

Table 1 shows a comparison of the stresses at the upper surface and in the center of the foundation at different points in time, obtained by the method proposed in [19], as well as by a simplified method at $\omega = 2/3$ and $\omega = 2/\pi$.

From Table 1 it can be seen that when approximating the temperature distribution curve over the thickness with a cosine wave ($\omega = 2/\pi$), the approximate technique better predicts maximum stresses at the initial time, and when approximating with a square parabola ($\omega = 2/3$), the approximate technique gives better results at the final time.

Table 1. Comparison of stresses at the top surface and in the center of the structure, calculated by the method presented in [19] and the simplified method.

t, Hours	σ_{up}, MPa			σ_{mid}, MPa		
	Method [19]	ω = 2/3	ω = 2/π	**Method [19]**	ω = 2/3	ω = 2/π
10	0.5907	0.6389	0.6101	−0.2900	−0.3195	−0.3483
20	0.8558	0.9676	0.9240	−0.5479	−0.4838	−0.5274
30	0.8587	1.0017	0.9565	−0.6022	−0.5008	−0.5460
40	0.7373	0.8935	0.8533	−0.5569	−0.4468	−0.4870
50	0.5625	0.7248	0.6922	−0.4709	−0.3624	−0.3951
60	0.3678	0.5331	0.5091	−0.3698	−0.2666	−0.2906
70	0.1702	0.3368	0.3217	−0.2652	−0.1684	−0.1836
80	−0.0216	0.1456	0.1390	−0.1630	−0.0728	−0.0793
90	−0.2027	−0.0357	−0.0340	−0.0661	0.0178	0.0194
100	−0.3710	−0.2044	−0.1952	0.0240	0.1022	0.1114
110	−0.5256	−0.3596	−0.3434	0.1068	0.1798	0.1960
120	−0.6666	−0.5012	−0.4786	0.1822	0.2506	0.2732
130	−0.7943	−0.6297	−0.6013	0.2505	0.3148	0.3432
140	−0.9095	−0.7456	−0.7120	0.3121	0.3728	0.4064
150	−1.0131	−0.8499	−0.8116	0.3674	0.4250	0.4633
160	−1.1060	−0.9436	−0.9011	0.4170	0.4718	0.5143
170	−1.1892	−1.0275	−0.9812	0.4614	0.5137	0.5600
180	−1.2637	−1.1025	−1.0528	0.5010	0.5512	0.6009
190	−1.3301	−1.1695	−1.1168	0.5364	0.5848	0.6375
200	−1.3895	−1.2294	−1.1740	0.5679	0.6147	0.6701

Based on a relation to (21), one can obtain the formula for the total stress on the upper surface at time t. To do this, let us omit the "up" index and write the stress increment in the form:

$$\Delta\sigma(\tau) = \frac{\partial\sigma(\tau)}{\partial\tau}d\tau = \frac{\omega E(\tau)}{1-\nu}\alpha\frac{\partial(\Delta T(\tau))}{\partial\tau}d\tau, \tag{23}$$

where $\Delta T(\tau) = T_{mid}(\tau) - T_{up}(\tau)$.

The total stress at time t is the sum of the increments over the time interval from τ_0 to t (τ_0 is the initial time):

$$\sigma(t) = \int_{\tau_0}^{t}\frac{\partial\sigma(\tau)}{\partial\tau}d\tau = \frac{\omega}{1-\nu}\alpha\int_{\tau_0}^{t}E(\tau)\frac{\partial(\Delta T(\tau))}{\partial\tau}d\tau. \tag{24}$$

Let us apply the integration-by-parts formula $\int udv = uv - \int vdu$ in (24), setting $u = E(\tau)$, $dv = \frac{\partial(\Delta T(\tau))}{\partial\tau}d\tau$. As a result, we obtain:

$$\sigma(t) = \frac{\omega\alpha}{1-\nu}\left(E(t)\Delta T(t) - E(\tau_0)\Delta T(\tau_0) - \int_{\tau_0}^{t}\Delta T(\tau)\frac{\partial(E(\tau))}{\partial\tau}d\tau\right). \tag{25}$$

Taking into account the fact that at the initial moment in time, there is no temperature difference between the center of the foundation and the surface ($\Delta T(\tau_0) = 0$), the final expression for the stress on the upper surface will take the form:

$$\sigma_{up}(t) = \frac{\omega\alpha}{1-\nu}\left(E(t)\Delta T(t) - \int_{\tau_0}^{t} \Delta T(\tau)\frac{\partial(E(\tau))}{\partial\tau}d\tau\right). \quad (26)$$

To obtain the stress formula in the center of the structure, it is sufficient to replace the factor ω in Formula (26) by $\omega - 1$. The coefficient $\omega/(1-\nu)$ can be denoted as the restraint coefficient k_T. Then, Formula (24) will take a form similar to (1) with the only exception that Formula (1) does not take into account the history of changes in the concrete elasticity modulus and temperature until the time t.

Based on Formula (21), one can also obtain a solution to the inverse problem, which is formulated as follows. For the given curves of change in time of the modulus of elasticity of concrete $E(t)$ and its tensile strength $R_t(t)$, it is required to find how the temperature difference ΔT between the center and the surface of the structure should change over time so that the stresses on the upper surface do not exceed R_t.

To construct a curve for the allowable value of $\Delta T(t)$, it is assumed that at each moment in time, the increment in stress on the upper surface is equal to the increment in tensile strength of concrete:

$$\Delta\sigma_{up} = \frac{\omega E(t)}{(1-\nu)}\alpha\{\Delta T(t) - \Delta T(t-\Delta t)\} = R_t(t) - R_t(t-\Delta t). \quad (27)$$

From (27) one can obtain a recursive formula for constructing the curve $\Delta T(t)$:

$$\Delta T(t) = \Delta T(t-\Delta t) + \frac{1-\nu}{\omega\alpha E(t)}[R_t(t) - R_t(t-\Delta t)]. \quad (28)$$

The curves constructed by Formula (28) at $\omega = 2/3$ и $\omega = 2/\pi$ are shown in Figure 11. When constructing these curves, the values of the modulus of elasticity of concrete and tensile strength were taken from the upper surface of the slab. Obviously, the allowable difference between the center and the surface of the structure is not a constant value, as postulated in [24,25], but depends on the age of the concrete.

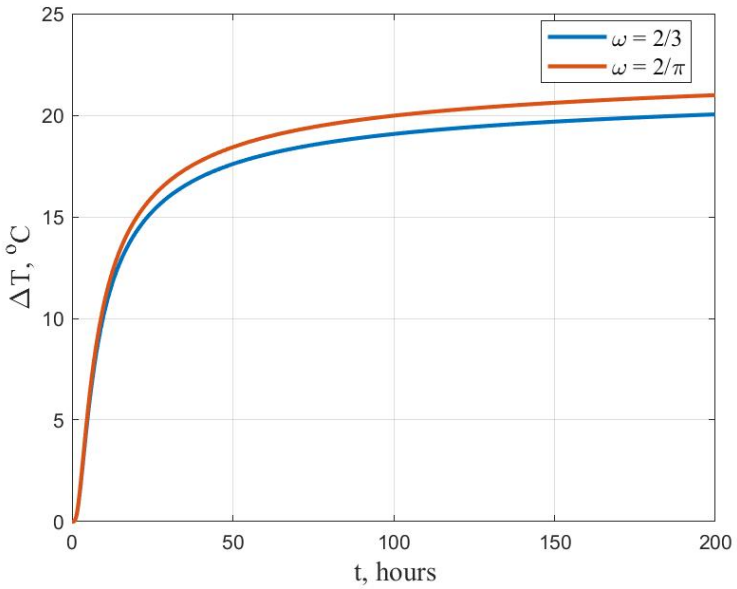

Figure 11. Change in time of the allowable temperature difference between the center and the surface of the structure.

Note that our calculations are still of an estimated nature, since Formula (16) gives reliable results when the age of concrete is more than 1 day. From Figure 2 it can be seen that at $t = 0$, the elastic modulus calculated by Formula (16) is not equal to zero. Although it should be very close to zero at the initial moment in time. Since the most intensive temperature increase occurs at the initial moment in time, the modulus of elasticity of concrete at an early age will have a significant impact on the resulting thermal stresses. Our further research will be aimed at clarifying the dependence of the elasticity modulus of concrete on time at an early age, as well as expanding the experimental base for temperature fields and stresses in hardening massive monolithic structures.

4. Conclusions

1. The approximate method for determining thermal stresses during the construction of massive monolithic foundation slabs is proposed based on the hypothesis of parabolic and cosine temperature distribution over the thickness of the structure. The introduced hypothesis made it possible to directly express the temperature stresses in terms of the difference between the center and the surface of the structure. The proposed method is quite simple and can be used for engineering calculations. It also allows one to assess the risk of early cracking based on field temperature measurements in the foundation slab.

2. The calculation dependences used are verified by comparison with experimental data for specimens hardening at 100% strain limitation.

3. It has been established that when using the cosine law of temperature distribution over the thickness, the approximate method better predicts the maximum stresses at the initial time, and in the case of a parabolic law, it gives better results for residual stresses.

4. The formula has been obtained that directly establishes the relationship between stresses and the temperature difference between the center and the surface, and also takes into account the history of changes in temperature and modulus of elasticity of concrete over time.

5. The inverse problem of determining the allowable temperature difference between the center and the surface of the foundation, which excludes early cracking of the concrete, has been solved. It is shown that the allowable temperature difference "center-surface" depends on the age of the concrete.

Author Contributions: Conceptualization, A.C. and V.T.; methodology, A.C.; software, V.T.; validation, A.C. and V.T.; formal analysis, A.C.; investigation, A.C.; resources, V.T.; data curation, V.T.; writing—original draft preparation, A.C.; writing—review and editing, V.T.; visualization, A.C.; supervision, A.C.; project administration, A.C.; funding acquisition, A.C. All authors have read and agreed to the published version of the manuscript.

Funding: This research received no external funding.

Data Availability Statement: This study did not report any data.

Acknowledgments: The authors would like to acknowledge the administration of Don State Technical University for their resources and financial support.

Conflicts of Interest: The authors declare no conflict of interest. The funders had no role in the design of the study; in the collection, analyses, or interpretation of data; in the writing of the manuscript; or in the decision to publish the results.

References

1. Chu, I.; Kwon, S.H.; Amin, M.N.; Kim, J.K. Estimation of temperature effects on autogenous shrinkage of concrete by a new prediction model. *Constr. Build. Mater.* **2012**, *35*, 171–182. [CrossRef]
2. Shen, D.; Wang, W.; Li, Q.; Yao, P.; Jiang, G. Early-age behaviour and cracking potential of fly ash concrete under restrained condition. *Mag. Concr. Res.* **2020**, *72*, 246–261. [CrossRef]
3. Safiuddin, M.; Kaish, A.A.; Woon, C.O.; Raman, S.N. Early-age cracking in concrete: Causes, consequences, remedial measures, and recommendations. *Appl. Sci.* **2018**, *8*, 1730. [CrossRef]
4. Shaikh, F.U.A. Effect of cracking on corrosion of steel in concrete. *Int. J. Concr. Struct. Mater.* **2018**, *12*, 3. [CrossRef]

5. Liu, J.; Tian, Q.; Wang, Y.; Li, H.; Xu, W. Evaluation method and mitigation strategies for shrinkage cracking of modern concrete. *Engineering* **2021**, *7*, 348–357. [CrossRef]
6. Xu, J.; Shen, Z.; Yang, S.; Xie, X.; Yang, Z. Finite element simulation of prevention thermal cracking in mass concrete. *Int. J. Comput. Sci. Math.* **2019**, *10*, 327–339. [CrossRef]
7. Huang, Y.; Liu, G.; Huang, S.; Rao, R.; Hu, C. Experimental and finite element investigations on the temperature field of a massive bridge pier caused by the hydration heat of concrete. *Constr. Build. Mater.* **2018**, *192*, 240–252. [CrossRef]
8. Abdel-Raheem, M.; Quintana, O.; Morales, M.; Marroquin-Villa, Y.; Ramos, D.; Hernandez, S. Construction methods used for controlling temperature in mass concrete structure. In Proceedings of the Creative Construction Conference 2018, Ljubljana, Slovenia, 30 June–3 July 2018; Budapest University of Technology and Economics: Budapest, Hungary, 2018; pp. 139–146.
9. Kanavaris, F.; Jędrzejewska, A.; Sfikas, P.I.; Schlicke, D.; Kuperman, S.; Šmilauer, V.; Honório, T.; Fairbairn, E.M.R.; Valentim, G.; de Faria, E.F.; et al. Enhanced massivity index based on evidence from case studies: Towards a robust pre-design assessment of early-age thermal cracking risk and practical recommendations. *Constr. Build. Mater.* **2021**, *271*, 121570. [CrossRef]
10. Maruyama, I.; Lura, P. Properties of early-age concrete relevant to cracking in massive concrete. *Cem. Concr. Res.* **2019**, *123*, 105770. [CrossRef]
11. Woo, H.M.; Kim, C.Y.; Yeon, J.H. Heat of hydration and mechanical properties of mass concrete with high-volume GGBFS replacements. *J. Therm. Anal. Calorim.* **2018**, *132*, 599–609. [CrossRef]
12. Newell, S.; Goggins, J. Investigation of thermal behaviour of a hybrid precasted concrete floor using embedded sensors. *Int. J. Concr. Struct. Mater.* **2018**, *12*, 66. [CrossRef] [PubMed]
13. Bushmanova, A.V.; Videnkov, N.V.; Semenov, K.V.; Dernakova, A.V.; Korovina, V.K. The thermo-stressed state in massive concrete structures. *Mag. Civ. Eng.* **2017**, *3*, 51–60.
14. Klemczak, B.; Batog, M.; Pilch, M.; Żmij, A. Analysis of cracking risk in early age mass concrete with different aggregate types. *Procedia Eng.* **2017**, *193*, 234–241. [CrossRef]
15. Nguyen, C.T.; Luu, X.B. Reducing temperature difference in mass concrete by surface insulation. *Mag. Civ. Eng.* **2019**, *4*, 70–79.
16. Van Lam, T.; Nguen, C.C.; Bulgakov, B.I.; Anh, P.N. Composition calculation and cracking estimation of concrete at early ages. *Mag. Civ. Eng.* **2018**, *6*, 136–148.
17. Mehta, P.K.; Monteiro, P.J.M. *Concrete: Microstructure, Properties, and Materials*; McGraw-Hill Education: New York, NY, USA, 2014.
18. Abbas, N.; Umar, T.; Salih, R.; Akbar, M.; Hussain, Z.; Haibei, X. Structural Health Monitoring of Underground Metro Tunnel by Identifying Damage Using ANN Deep Learning Auto-Encoder. *Appl. Sci.* **2023**, *13*, 1332. [CrossRef]
19. Chepurnenko, A.; Nesvetaev, G.; Koryanova, Y.; Yazyev, B. Simplified model for determining the stress-strain state in massive monolithic foundation slabs during construction. *Int. J. Comput. Civ. Struct. Eng.* **2022**, *18*, 126–136.
20. Nesvetaev, G.V.; Koryanova, Y.I.; Chepurnenko, A.S.; Sukhin, D.P. On the issue of modeling thermal stresses during concreting of massive reinforced concrete slabs. *Eng. J. Don* **2022**, *6*, 375–394. Available online: http://ivdon.ru/en/magazine/archive/n6y2022/7691 (accessed on 23 April 2023).
21. Bjøntegaard, Ø. Basis for and Practical Approaches to Stress Calculations and Crack risk Estimation in Hardening Concrete structures–State of the Art. FA 3 Technical Performance. SP 3.1 Crack Free Concrete Structures. 2011. Available online: https://sintef.brage.unit.no/sintef-xmlui/bitstream/handle/11250/2411102/coin31.pdf?sequence=1 (accessed on 23 April 2023).
22. Nesvetaev, G.V.; Koryanova, Y.I.; Chepurnenko, A.S.; Sukhin, D.P. Evaluation of some methods for calculating thermal stresses during concreting of massive reinforced concrete foundation slabs. *Eng. J. Don* **2022**, *7*, 438–454. Available online: http://ivdon.ru/en/magazine/archive/n7y2022/7817 (accessed on 23 April 2023).
23. Chepurnenko, A.S.; Nesvetaev, G.V.; Koryanova, Y.I. Modeling non-stationary temperature fields when constructing mass cast-in-situ reinforced-concrete foundation slabs. *Archit. Eng.* **2022**, *7*, 66–78. Available online: https://aej.spbgasu.ru/index.php/AE/article/view/601 (accessed on 23 April 2023). [CrossRef]
24. Rahimi, A.; Noorzaei, J. Thermal and structural analysis of roller compacted concrete (RCC) dams by finite element code. *Aust. J. Basic Appl. Sci.* **2011**, *5*, 2761–2767.
25. Bofang, Z. *Thermal Stresses and Temperature Control of Mass Concrete*; Butterworth-Heinemann: Oxford, UK, 2014.